HHS Public Access

Author manuscript

Chem Commun (Camb). Author manuscript; available in PMC 2016 August 04.

Published in final edited form as:

Chem Commun (Camb). 2015 August 4; 51(60): 12028–12031. doi:10.1039/c5cc04251h.

Selective targeting of *Mycobacterium smegmatis* with trehalose-functionalized nanoparticles†

Kalana W. Jayawardana[a], **H. Surangi N. Jayawardena**[a,b], **Samurdhi A. Wijesundera**[a], **Thareendra De Zoysa**[a], **Madanodaya Sundhoro**[a], and **Mingdi Yan**[a]

Mingdi Yan: mingdi_yan@uml.edu

[a]Department of Chemistry, University of Massachusetts Lowell, Lowell, MA 01854, USA. Fax: +1-978-934-3013; Tel: +1-978-934-3647

[b]David H. Koch Institute for Integrative Cancer Research Centre, Massachusetts Institute of Technology, Cambridge, MA 02139, USA

Abstract

Silica and iron oxide nanoparticles with sizes ranging from 6 to 40 nm were functionalized with trehalose. The trehalose-conjugated nanoparticles showed strong interactions with *Mycobacterium smegmatis* (*M. smegmatis*) and minimal interactions with macrophage (RAW 264.7) or A549 cells. In addition, trehalose-conjugated silica nanoparticles selectively interacted with *M. smegmatis* on *M. smegmatis*-treated A549 cells, demonstrating high potential of trehalose in developing targeted therapy for treating mycobacterial infection.

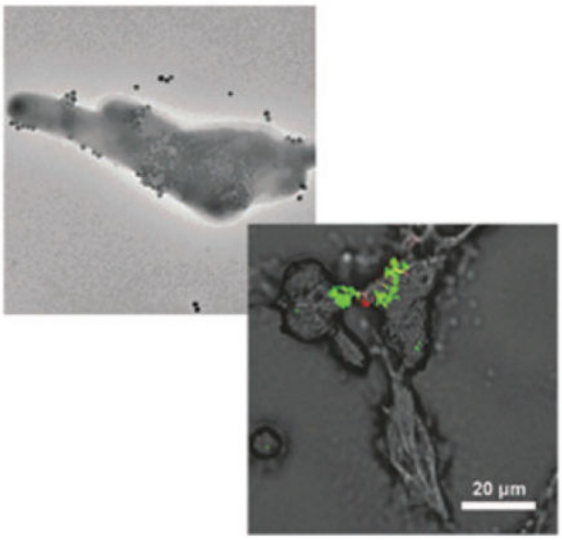

†Electronic supplementary information (ESI) available: Experimental details of the synthesis, functionalization, TEM, DLS and TGA characterization of nanoparticles, carbohydrate density measurement, TEM sample preparation and additional TEM images, SEM images and cell viability data. See DOI: 10.1039/ c5cc04251h

Correspondence to: Mingdi Yan, mingdi_yan@uml.edu.

With an estimated 9 million new cases each year, and 1.5 million fatalities in 2013, TB, an infectious disease caused by *Mycobacterium tuberculosis*, is among the most widespread diseases to plague mankind.[1] The resurgence of TB especially the drug-resistant TB in recent years calls for the development of new diagnostic and therapeutic strategies.[2] TB poses additional challenges owing to the unique structure of mycobacteria. The mycobacterial cell wall resembles that of the Gram-positive bacteria; however, it has an additional layer of lipids. This lipid-rich cell wall acts as a permeability barrier to polar molecules and controls the passage of host susceptibility components such as antimicrobial drugs into the cell.[3] Relatively hydrophobic antibiotics such as rifampicin and fluoroquinolones are able to diffuse through the lipid bilayer; however, only a small number of hydrophilic antibiotics can cross the bilayer through porin channels due to low abundance of mycobacterial porins on the outer membrane.[4]

This issue can potentially be overcome by using nanomaterial-based therapeutics to deliver antimicrobial drugs. Efficient uptake of nanomaterials by the cells is the first step for the effective delivery of drugs and therapeutic agents.[5–8] Internalization of nanoparticles by mammalian cells has been well documented, leading to the conclusion of receptor-mediated endocytosis for the uptake of nanoparticles by mammalian cells.[9–11] For bacterial cells, however, the general view does not support endocytosis, pinocytosis or exocytosis due to the presence of the thick peptidoglycan cell wall.[12–14] Therefore, methods facilitating the targeting of bacterial cells are of high importance in developing effective antimicrobial nanotherapeutics.

In this work, we report a general strategy to target mycobacteria by conjugating trehalose with nanoparticles. Trehalose is a non-mammalian disaccharide and is a major component in the cytosol of both *M. smegmatis* and *M. tuberculosis*, making up 1.5–3% of the bacterial dry weight.[15,16] Trehalose is also incorporated into a range of mycobacterial cell wall glycolipids (*e.g.* trehalose 6,6′-dimycolate),[16,17] which participate in cell wall associated pathogenicity of *M. tuberculosis*.[18] Exogenous trehalose is transported to the mycobacterial cytoplasm through the high affinity trehalose transporter system.[19] The prominence of trehalose in the cytoplasm and the role that it plays towards pathogenicity have led to drug targets that can be used to disrupt trehalose biosynthesis pathways in *M. tuberculosis*.[20] In the work of Davis and coworkers,[21] trehalose labeled with a fluorescent dye was used as an imaging probe to detect *M. tuberculosis in vitro*, where the dye-trehalose conjugate was internalized by the mycobacterium bacilli through the trehalose transporter.

Nanoparticles used in this study include silane-protected iron oxide magnetic nanoparticles (MNPs), silica nanoparticles (SNPs), and fluorescein (FITC)-doped silica nanoparticles (FSNPs). MNPs were prepared by heating iron(III) acetylacetonate, 1,2-hexadecanediol, oleic acid and oleylamine in dibenzyl ether, and were silanized with 3-(trihydroxysilyl)propyl methyl-phosphonate, monosodium salt (phosphonate-silane) to increase the water dispersibility (Scheme S1, ESI†).[22] Particle sizes were measured to be 6.4

†Electronic supplementary information (ESI) available: Experimental details of the synthesis, functionalization, TEM, DLS and TGA characterization of nanoparticles, carbohydrate density measurement, TEM sample preparation and additional TEM images, SEM images and cell viability data. See DOI: 10.1039/ c5cc04251h

± 0.7 nm (TEM) or 6.7 ± 0.6 nm (DLS) (Fig. S1, ESI†). SNPs were synthesized using a modified Stöber method,[23] and the particle size was 42.1 ± 1.9 nm (TEM) or 44.4 ± 1.7 nm (DLS) (Fig. S2, ESI†). FSNPs were prepared by co-condensing tetraethyl orthosilicate with FITC-derivatized silane,[24,25] and the particle size was 30.2 ± 2.1 nm (TEM) or 32.9 ± 1.9 nm (DLS) (Fig. S3, ESI†). Trehalose was conjugated with nanoparticles using the photocoupling chemistry developed in our laboratory.[26–30] Nanoparticles were first functionalized with perfluorophenyl azide (PFPA) by treating SNPs or FSNPs with silane-derivatized PFPA,[31–34] or MNPs with a phosphate-derivatized PFPA (Scheme S1, see ESI† for details).[35,36] The resulting PFPA-NPs (Fig. S4, ESI†) showed the asymmetric stretch of the azide ($-N_3$) at ~2119 cm^{-1} in the FTIR spectra (Fig. S5, ESI†). Trehalose was then covalently conjugated with PFPA-NPs by irradiating the particles in the presence of an aqueous solution of trehalose (Fig. S6 and Scheme S1, ESI†).[35,37,38] The density of trehalose conjugated with nanoparticles was determined by thermogravimetric analysis (TGA) to be 11.5×10^{-16}, 4.1×10^{-16}, 8.7×10^{-16} μg nm^{-2} for Tre-SNPs, Tre-MNPs and Tre-FSNPs, respectively (Fig. S7 and Table S1, ESI†). D-Glucose (Glc), β-cyclodextrin (CD) and maltoheptaose (G7) were used as controls and were conjugated with nanoparticles following the same protocol as trehalose. The densities of these carbohydrates conjugated with nanoparticles, determined by TGA, were on the same order of magnitude as those of trehalose (Table S1, ESI†).

M. smegmatis was used as the model mycobacterium[39–41] because it has been widely accepted as a mycobacterium model for the development of therapeutic drugs against TB[42–45] and it is non-pathogenic. In the experiment, carbohydrate-conjugated nanoparticles were treated with *M. smegmatis* at 37 °C for 6 h. After excess nanoparticles were removed from the medium, the samples were examined under TEM. Results showed that nanoparticles conjugated with Tre had higher interactions with *M. smegmatis* than nanoparticles modified with G7 or CD (Fig. 1a). Particles were pressed against the cell wall, creating crevices on the bacilli.

Thin section samples prepared from the bacteria treated with Tre-MNPs showed the presence of nanoparticles in the cytoplasm of *M. smegmatis* (Fig. 2a and Fig. S8, ESI†). Similar observations were obtained with nanoparticles conjugated with Glc where particles were seen on the surface (Fig. 1b) as well as inside the bacterial cells (Fig. 2b). For nanoparticles conjugated with G7 or CD, however, very little surface adherence was observed on the bacteria (Fig. 1c and d). Furthermore, no particles were observed inside *M. smegmatis* from the thin section samples (Fig. 2c and d).

We next investigated the interactions of carbohydrate-conjugated nanoparticles with mammalian cells. In this case, FSNPs, which fluoresce green, were used to aid visualization. Tre-FSNPs were incubated with murine macrophage (RAW 264.7) in serum free DMEM medium at 37 °C for 2 h, and the sample was then treated with nucleic acid staining dye SYTO 61®. Laser scanning confocal microscopy (LSCM) images show that samples treated with Tre-FSNPs were mostly red, which is the color of the stained macrophages (Fig. 3a). On the other hand, samples treated with Glc-FSNPs under the same conditions appeared orange (Fig. 3b), which is the mix of red (labeled macrophages) and green (FSNPs). This demonstrates that Tre-conjugated nanoparticles had little interactions with the macrophage

whereas Glc-conjugated nanoparticles interacted strongly with the macrophage. The experiment was repeated using A549 cells and Tre- or Glc-conjugated iron oxide nanoparticles. The samples were stained with potassium ferricyanide to detect the presence of iron. A549 cells treated with Tre-MNPs showed minimal color whereas cells treated with Glc-MNPs showed the typical Prussian blue color (Fig. S9, ESI†). These results are consistent with those from the macrophage study that Tre-conjugated nanoparticles had little interactions with the cells whereas Glc-NPs interacted strongly with both cell lines.

The viability of *M. smegmatis* after treating with carbohydrate-conjugated SNPs was tested by the alamarBlue® assay. Cell viabilities of 98%, 96%, 97% and 98% were obtained for Tre-SNPs, Glc-SNPs, G7-SNPs and CD-SNPs, respectively (Fig. S10a, ESI†). For A549 cells, the WST-8 assay[46] was used and cell viabilities of 99%, 99%, 78%, 98%, 98% and 85% were obtained for Tre-SNPs, Glc-SNPs, CD-SNPs, G7-SNPs, Tre-FSNPs and CD-FSNPs, respectively (Fig. S10b, ESI†). These results suggest low toxicity of carbohydrate-conjugated SNPs towards the mycobacteria and A549 cells under the experimental conditions.

The selective interaction of Tre-NPs with *M. smegmatis* over mammalian cells opens up the possibility of using trehalose as the targeting ligand for mycobacteria. To further confirm the selectivity of trehalose-mediated interactions towards mycobacteria, A549 cells were treated with SYTO® 61-stained *M. smegmatis* and fixed in paraformaldehyde (5%) solution. The mycobacteria (fluoresce red) were seen on A549 cells in both (LSCM) images (Fig. 4a) and the SEM image (Fig. S11a, ESI†). *M. smegmatis*-treated A549 cells were then incubated with Tre-FSNPs for 6 h. The LSCM image showed the green color (Tre-FSNPs) in the region of the A549 cells that had *M. smegmatis* (Fig. 4b). In the SEM image, nanoparticles were also observed on A549 cells where *M. smegmatis* were present (Fig. S11b, ESI†). In addition, the optical image (Fig. 4c) merged with the LSCM images showed Tre-FSNPs (green) in the regions where *M. smegmatis* (red) were present (Fig. 4d). In the control experiment where the *M. smegmatis*-treated A549 cells were incubated with CD-FSNPs, no green color was seen in the LSCM image (Fig. S12, ESI†) and no nanoparticles were observed on the bacteria in the SEM image either (Fig. S11c, ESI†). These results further supported that trehalose-mediated interactions are specific towards mycobacteria and are selective over mammalian cells.

In summary, we have demonstrated that nanoparticles conjugated with trehalose exhibit strong interactions with *M. smegmatis*. TEM thin section images revealed the presence of Tre-MNPs on the cell wall as well as in the cytoplasm of *M. smegmatis*. Furthermore, Tre-NPs had minimal interactions with macrophage (RAW 264.7) or A549 cells. When Tre-NPs were incubated with A549 cells treated with *M. smegmatis*, Tre-NPs were found only in the regions where *M. smegmatis* were present.

This selective interaction with *M. smegmatis* over mammalian cells was absent in Glc-NPs where the nanoparticles showed high interactions with both *M. smegmatis* and mammalian cells. The general strategy of using trehalose-facilitated interactions with mycobacteria has high potential in developing effective therapeutic and diagnostic tools for treating mycobacterial infections such as TB.

Supplementary Material

Refer to Web version on PubMed Central for supplementary material.

Acknowledgments

This work was supported by NIH (R01GM080295 and R21AI109896), and a startup fund from University of Massachusetts Lowell. The authors thank Mr. Christopher Santeufemio for his assistance in the preparation of TEM thin section samples.

Notes and references

1. World Health Organization. Geneva, Switzerland: 2014.
2. Mehanna MM, Mohyeldin SM, Elgindy NA. J Controlled Release. 2014; 187:183–197.
3. Daffe M, Etienne G. Tubercle. 1999; 79:153–169.
4. Lambert PA. J Appl Microbiol. 2002; 92:46S–54S. [PubMed: 12000612]
5. Wang AZ, Langer R, Farokhzad OC. Annu Rev Med. 2012; 63:185–198. [PubMed: 21888516]
6. Petros RA, De SJM. Nat Rev Drug Discovery. 2010; 9:615–627. [PubMed: 20616808]
7. Li Y, Hindi K, Watts KM, Taylor JB, Zhang K, Li Z, Hunstad DA, Cannon CL, Youngs WJ, Wooley KL. Chem Commun. 2010; 46:121–123.
8. Davis ME, Chen Z, Shin DM. Nat Rev Drug Discovery. 2008; 7:771–782. [PubMed: 18758474]
9. Canton I, Battaglia G. Chem Soc Rev. 2012; 41:2718–2739. [PubMed: 22389111]
10. Walczyk D, Bombelli FB, Monopoli MP, Lynch I, Dawson KA. J Am Chem Soc. 2010; 132:5761–5768. [PubMed: 20356039]
11. Wang M, Thanou M. Pharmacol Res. 2010; 62:90–99. [PubMed: 20380880]
12. Lonhienne TGA, Sagulenko E, Webb RI, Lee KC, Franke J, Devos DP, Nouwens A, Carroll BJ, Fuersta JA. Proc Natl Acad Sci U S A. 2010; 107:12883–12888. [PubMed: 20566852]
13. Kloepfer JA, Mielke RE, Nadeau JL. Appl Environ Microbiol. 2005; 71:2548–2557. [PubMed: 15870345]
14. Kumar A, Pandey AK, Singh SS, Shanker R, Dhawan A. Cytometry, Part A. 2011; 79:707–712.
15. Elbein D, Mitchell M. J Bacteriol. 1973; 113:863–873. [PubMed: 4632324]
16. Woodruff PJ, Carlson BL, Siridechadilok B, Pratt MR, Senaratne RH, Mougous JD, Riley LW, Williams SJ, Bertozzi CR. J Biol Chem. 2004; 279:28835–28843. [PubMed: 15102847]
17. Hoffmann C, Leis A, Niederweis M, Plitzko JM, Engelhardt H. Proc Natl Acad Sci U S A. 2008; 105:3963–3967. [PubMed: 18316738]
18. Yamagami H, Matsumoto T, Fujiwara N, Arakawa T, Kaneda K, Yano I, Kobayashi K. Infect Immun. 2001; 69:810–815. [PubMed: 11159972]
19. Kalscheuer R, Weinrick B, Veeraraghavan U, Besra GS, Jacobs WR. Proc Natl Acad Sci U S A. 2010; 107:21761–21766. [PubMed: 21118978]
20. Nobre A, Alarico S, Maranha A, Mendes V, Empadinhas N. Microbiology. 2014; 160:1547–1570. [PubMed: 24858083]
21. Backus KM, Boshoff HI, Barry CS, Boutureira O, Patel MK, D'Hooge F, Lee SS, Via LE, Tahlan K, Barry CE III, Davis BG. Nat Chem Biol. 2011; 7:228–235. [PubMed: 21378984]
22. Jayawardena HSN, Jayawardana KW, Chen X, Yan M. Chem Commun. 2013; 49:3034–3036.
23. Wang X, Ramstrom O, Yan M. Analyst. 2011; 136:4174–4178. [PubMed: 21858301]
24. Wang X, Ramstrom O, Yan M. Chem Commun. 2011; 47:4261–4263.
25. Gann JP, Yan M. Langmuir. 2008; 24:5319–5323. [PubMed: 18433181]
26. Chen X, Ramstrom O, Yan M. Nano Res. 2014; 7:1381–1403. [PubMed: 26500721]
27. Liu LH, Yan M. Acc Chem Res. 2010; 43:1434–1443. [PubMed: 20690606]
28. Park J, Yan M. Acc Chem Res. 2013; 46:181–189. [PubMed: 23116448]
29. Wang X, Ramstroem O, Yan M. Adv Mater. 2010; 22:1946–1953. [PubMed: 20301131]

30. Wang X, Liu LH, Ramstrom O, Yan M. Exp Biol Med. 2009; 234:1128–1139.
31. Wang X, Matei E, Deng L, Koharudin L, Gronenborn AM, Ramstrom O, Yan M. Biosens Bioelectron. 2013; 47:258–264. [PubMed: 23584388]
32. Wang H, Li LL, Tong Q, Yan MD. ACS Appl Mater Interfaces. 2011; 3:3463–3471. [PubMed: 21834589]
33. Tong Q, Wang X, Wang H, Kubo T, Yan M. Anal Chem. 2012; 84:3049–3052. [PubMed: 22385080]
34. Wang H, Ren J, Hlaing A, Yan M. J Colloid Interface Sci. 2011; 354:160–167. [PubMed: 21044787]
35. Liu LH, Dietsch H, Schurtenberger P, Yan M. Bioconjugate Chem. 2009; 20:1349–1355.
36. Xu C, Uddin KMA, Shen X, Surangi H, Jayawardena N, Yan M, Ye L. ACS Appl Mater Interfaces. 2013; 5:5208–5213. [PubMed: 23673293]
37. Wang X, Matei E, Gronenborn AM, Ramstrom O, Yan M. Anal Chem. 2012; 84:4248–4252. [PubMed: 22548468]
38. Wang X, Matei E, Deng L, Ramstroem O, Gronenborn AM, Yan M. Chem Commun. 2011; 47:8620–8622.
39. Ofer N, Wishkautzan M, Meijler M, Wang Y, Speer A, Niederweis M, Gur E. Appl Environ Microbiol. 2012; 78:7483–7486. [PubMed: 22885758]
40. Shiloh MU, DiGiuseppe Champion PA. Curr Opin Microbiol. 2010; 13:86–92. [PubMed: 20036184]
41. Fujiwara N, Naka T, Ogawa M, Yamamoto R, Ogura H, Taniguchi H. Tuberculosis. 2012; 92:187–192. [PubMed: 22056691]
42. Titgemeyer F, Amon J, Parche S, Mahfoud M, Bail J, Schlicht M, Rehm N, Hillmann D, Stephan J, Walter B, Burkovski A, Niederweis M. J Bacteriol. 2007; 189:5903–5915. [PubMed: 17557815]
43. Jin J, Zhang JY, Guo N, Sheng H, Li L, Liang JC, Wang XL, Li Y, Liu MY, Wu XP, Yu L. Molecules. 2010; 15:7750–7762. [PubMed: 21042264]
44. Rodrigues L, Ramos J, Couto I, Amaral L, Viveiros M. BMC Microbiol. 2011; 11:35. [PubMed: 21332993]
45. Lu P, Lill H, Bald D, Villellas C, Koul A, Andries K. J Antibiot. 2014
46. Liong M, Lu J, Kovochich M, Xia T, Ruehm SG, Nel AE, Tamanoi F, Zink JI. ACS Nano. 2008; 2:889–896. [PubMed: 19206485]

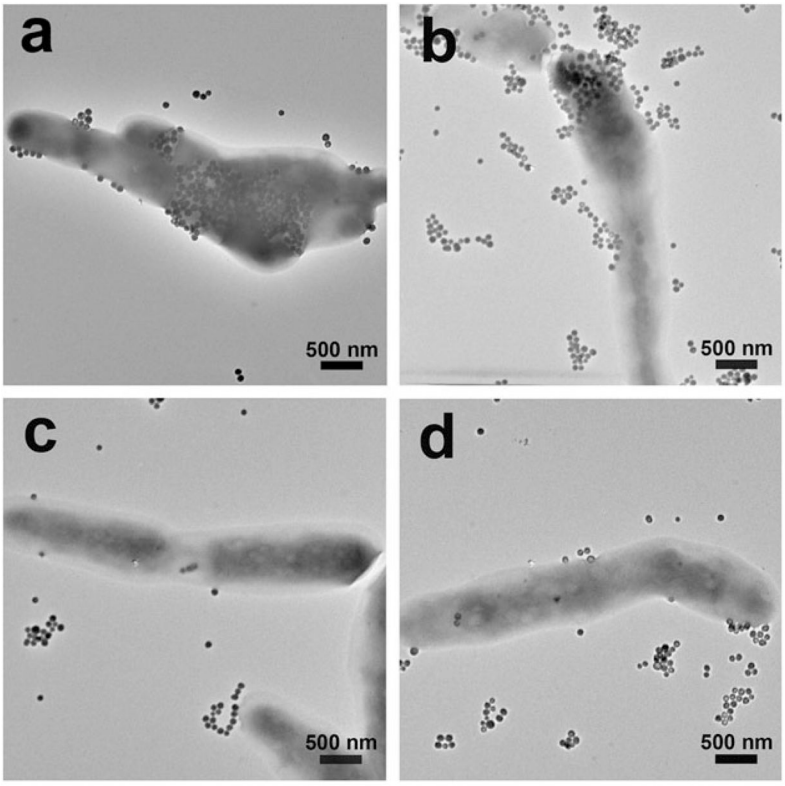

Fig. 1.

TEM images of *M. smegmatis* strain mc^{2}155 after incubating for 6 h with (a) Tre-SNP, (b) Glc-SNPs, (c) G7-SNPs, and (d) CD-SNPs.

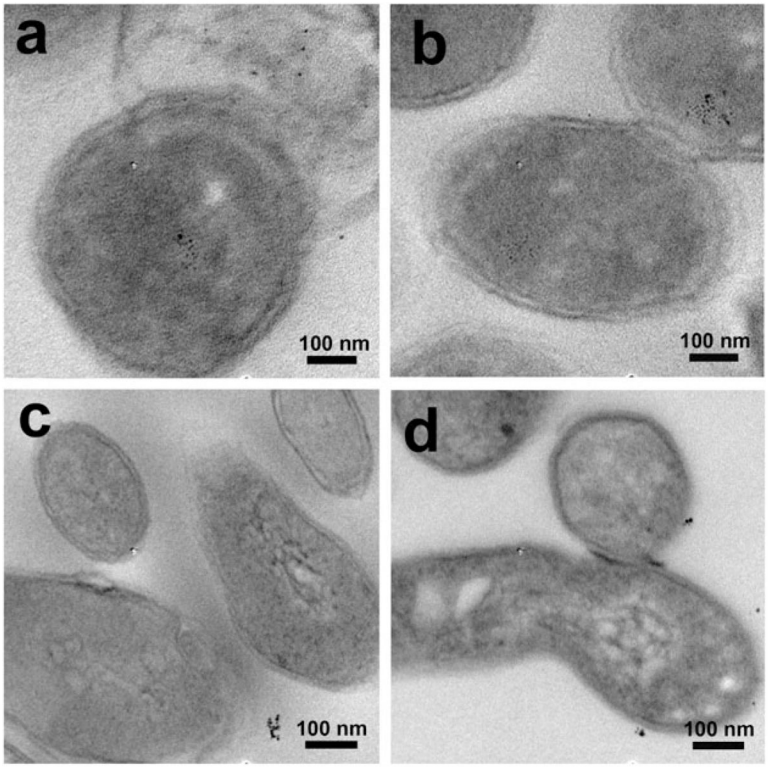

Fig. 2.

TEM images of thin section samples of *M. smegmatis* (mc^2155) after incubating for 6 h with (a) Tre-MNPs, (b) Glc-MNPs, (c) G7-MNPs, and (d) CD-MNPs.

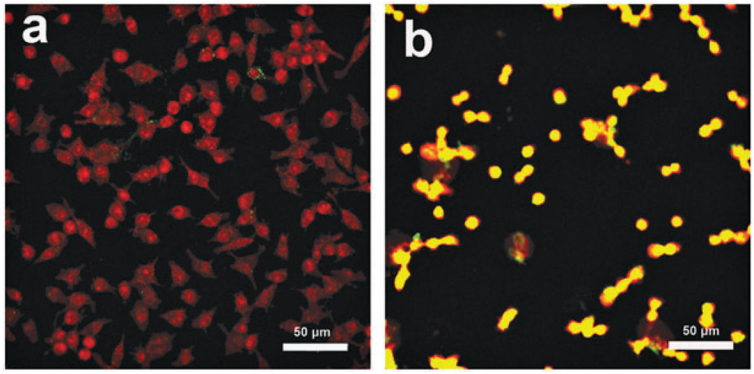

Fig. 3.

LSCM overlay images of murine macrophages (RAW 264.7) stained with SYTO® 61 after incubation with (a) Tre-FSNPs and (b) Glc-FSNPs.

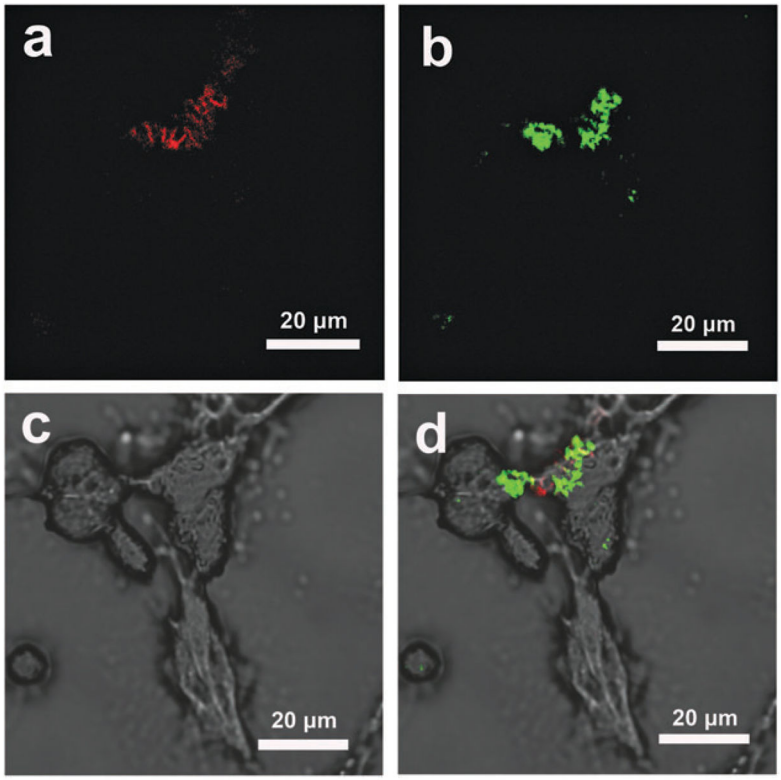

Fig. 4.

M. smegmatis -treated A549 cells incubated with Tre-FSNPs. *M. smegmatis* was stained with SYTO® 61 dye which fluoresces red. FSNPs were doped with FITC which fluoresces green. (a) LSCM image at 633 nm excitation showing SYTO® 61-stained *M. smegmatis*. (b) LSCM image at 488 nm excitation showing Tre-FSNPs. (c) Optical image of *M. smegmatis*-treated A549 cells (d) merged image of the optical (c) and LSCM (a, b) images showing Tre-FSNPs (green) clustered on top of *M. smegmatis* (red).